PHYSICAL REVIEW E **88**, 052310 (2013)

Kinetics of anisotropic ordering in Laponite dispersions induced by a water-air interface

Ravi Kumar Pujala[1] and H. B. Bohidar[1,2,*]
[1]*School of Physical Sciences, Jawaharlal Nehru University, New Delhi-110067, India*
[2]*Special Center for Nanosciences, Jawaharlal Nehru University, New Delhi-110067, India*

(Received 19 June 2013; revised manuscript received 5 September 2013; published 20 November 2013)

In this work, we report the kinetics of ordering occurring at the water-air interface of Laponite dispersions. Propagation of such ordering into the bulk and its relaxation dynamics were systematically studied through light scattering measurements. Depolarization ratio D_p, which accounted for the optical anisotropy, was measured as a function of depth from the interface and aging of the samples. The extent of spatial ordering was found to be several decades larger than the typical particle size. Spatial ordering originated from the interface and percolated into the bulk with aging time t_w. Growth in D_p with waiting time was found to follow power-law behavior given as $D_p \sim t_w^n$, with n increasing from 0.1 to 4 as one moved away from the interface into the bulk. D_p decreased exponentially with depth h given as $D_p \sim e^{-(h/h_0)}$, where h_0 is the decay length, increasing from 0.4 to 0.75 mm with aging time. Dynamic structure factor measurements performed on the samples at various aging times, depths, and temperatures yielded two distinct relaxation times: one fast mode followed by a slow mode. The fast mode remained invariant while slow mode relaxation time followed an exponential decay with depth. This study indicated that the arrested phase nucleated from the interface and propagated into the bulk, which was not observed when the surface was insulated with a layer of hydrophobic liquid. Dilution of the concentrated samples destroyed the aforesaid ordering and made the dispersion homogeneous implying the ordered state was a glass.

DOI: 10.1103/PhysRevE.88.052310 PACS number(s): 82.70.Dd, 64.70.pv, 81.05.Xj, 64.70.Nd

I. INTRODUCTION

Many interesting phenomena occurring in material science are caused at the interface of different fluids [1–4], the water-air interface being the most common among them. Clay dispersions are very interesting soft matter systems that produce various concentration and age dependent arrested phases, which are of both industrial and scientific importance. The nontrivial phase diagrams exhibited by these dispersions owe their existence to the anisotropy associated with the geometrical shape and electrical charge of these discotic particles.

Colloidal clays have recently emerged as complex model systems with a very rich phase diagram, encompassing fluid, gel, and glassy states [5–14]. Often these disordered phases are found to interfere with ordered ones, namely nematic and columnar phases. Aging is the most commonly observed feature in disordered states of matter such as colloidal gels and glasses. Glassy materials are not entirely frozen, but continue to relax at slower and slower rates as they age towards equilibrium. The phenomenon of aging in clay dispersions is under intense investigation by several research groups [15–21] and it continues to yield interesting features, which are helpful in understanding the complexities observed in biological systems. The effect of temperature is clearly manifested in the properties of soft matter systems. Recently, Hansen *et al.* observed the swelling transition in passive clay systems induced by heating [22]. Temperature induced orientational ordering in the mixed clay dispersions was reported by us in a previous study [23].

The phenomenon of dynamic arrest is clearly observed in clay dispersions which have been extensively probed [8,9,13,20,21]. Several mechanisms for dynamic arrest have been identified and a rich phenomenology has been predicted both at a high reentrant liquid-glass line, attractive and repulsive glasses, and at low clay concentrations where gelation was shown to occur from different thermodynamic routes. Recently, the existence of equilibrium gels in systems with intrinsic anisotropy (patchy colloids) has been observed from experimental and numerical studies [11].

Laponite is an entirely synthetic layered silicate that is widely used as a rheology modifier in industrial applications such as paints, varnishes, cosmetics, and polymer nanocomposites [24,25]. For investigating the formation of multiple arrested states, charged colloidal clays made of nanometer-sized discotic platelets have emerged as suitable candidates. The structural anisotropy associated with the clay particles, combined with the presence of attractive and repulsive terms in their interparticle interactions, causes the complexity observed in the phase diagram of such colloidal systems. In particular, Laponite displays a nontrivial aging dynamics replete with multiple arrested states.

There have been many reports on the study of orientational ordering of clays [26–30]. Recently, the phenomenon of the interface induced ordering was observed by Shahin *et al.* in Laponite suspensions using optical birefringence studies [26]. An important question arises here: How does the interface affect the particle dynamics and its ordering? Herein, we address this issue by collecting information from a series of controlled experiments performed on aging Laponite dispersions. We report on the ordering of Laponite platelets as the dispersion develops optical anisotropy starting at the water-air interface. This ordering propagates into the bulk over many orders of magnitude compared to the platelet size with aging time. We have used depolarized laser light scattering to investigate this ordering process quantitatively and further studied the relaxation dynamics from dynamic structure factor measurements. We found the existence of correlation between

---

[*] Corresponding author: bohi0700@mail.jnu.ac.in

©2013 American Physical Society

the ordering and the relaxation time with aging, temperature, and depth of the sample measured from the interface. The effect of insulation of the water-air interface, temperature, and aging time on the aforesaid phenomenon was also studied systematically. Interestingly, the hydrophobic insulation of the interface destroyed the phenomenon of ordering.

II. MATERIALS AND METHODS

Laponite RD clay was purchased from Southern Clay Products, USA. We dried the Laponite clay for 4 h at 120 °C to remove the moisture present. Laponite dispersions were prepared following the exact protocol described in Ref. [31] using de-ionized water at room temperature, 25 °C. The dispersions were filtered through 0.45-μm Millipore filter and the pH was adjusted to 10. Dispersions appeared optically clear and transparent.

Depolarized light scattering (DPLS) experiments were performed on a 256-channel digital correlator (PhotoCor Instruments, USA) that was operated in the multi-tau mode (logarithmically spaced channels). The time scale spanned over eight decades, i.e., from 0.5 μs to 10 s. This instrument used a 35-mW linearly polarized He:Ne laser. A Glan Thomson analyzer was used in front of the photomultiplier tube to enable collection of polarized and depolarized components of scattered light (I_{VV} and I_{VH}). The probe length scale is defined by the inverse of the modulus of the scattering wave vector q where the wave vector $q = (4\pi n/\lambda)\sin(\theta/2)$, the medium refractive index is n, excitation wavelength is λ (632.8 nm), and θ is the scattering angle. The scattered intensity values were measured at the scattering angle 90°. Further details on depolarized light scattering can be obtained from Ref. [32].

The experiment required that scattered light was to be collected from different sample depths with respect to the water-air interface. Since in a standard goniometer geometry attached to a light scattering spectrometer it is not possible to collect scattered light emanating from various sample depths, we had to make a precision sample holder and adapt it to the sample compartment of the goniometer.

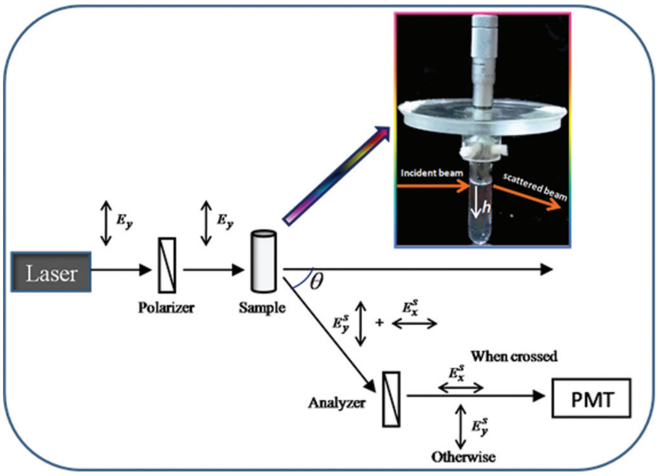

FIG. 1. (Color online) Schematic illustration of the setup used to study the height dependent growth of anisotropy in the system. The sample holder, micrometer screw jack, and the sample are shown in the inset.

It contained the micrometer screw jack mounted on a disk shaped structure as shown in Fig. 1. The screw jack was connected to a cylindrical neck below the circular disk. The top of the cylindrical glass cell which contained the sample could be inserted into this neck and fastened with three symmetrically placed Teflon screws. This placed the sample cell firmly inside the scattering chamber of the goniometer. The jack was calibrated with the main scales and 25 circular scales. This meant that the jack was capable of producing fine rotational as well as the translational displacement. By moving the jack in a clockwise direction we could move the sample downwards whereas its anticlockwise motion lifted the sample in an upward direction. Therefore, the rotational as well as the translational displacement of the sample was possible that was required for our inspection as we wanted to observe the anisotropy as a function of depth from the interface to bulk inside the sample. This arrangement facilitated the vertical displacement of the cell with the precision of 0.255 μm which was the least count of the jack. Thus, the displacements caused during the measurements were extremely precise. A built-in temperature controller was used to control the temperature during the experiments which was fixed to 25 °C in our case.

The analyzer was kept at a right angle to the direction of the propagation of the laser light so as to minimize the effect of the stray light, and the presence of an interference filter ensured that the signal to noise ratio was robust. The angle in the analyzer was adjusted either to 0° or 90°, respectively, as per the requirement. The zero degree alignment of the analyzer meant that only the parallel component (I_{VV}) of the scattered light passed through it to the detector whereas the 90° alignment of the analyzer ensured passage of only the perpendicular component (I_{VH}) of the scattered light. The depolarization ratio is defined as follows [32]:

$$D_p = \frac{I_{VH}}{I_{iso}}, \tag{1}$$

and

$$I_{iso} = I_{VV} - \tfrac{4}{3} I_{VH}, \tag{2}$$

where I_{VH} and I_{VV} are the depolarized and polarized components of the scattered intensity.

III. EXPERIMENTAL RESULTS

A. Anisotropic ordering at the water-air interface

In this work, we report on Laponite suspensions that developed optical anisotropy over many days while exhibiting transformation into a completely jammed state. The geometrical anisotropy associated with the scattering particles depolarizes the incident light, and the scattered electrical field can be decomposed into the parallel $E_{VV}(q,t)$ and perpendicular $E_{VH}(q,t)$ components, with respect to the direction of the incident polarization. These quantities fluctuate due to the random translational and rotational motion of the particles, and one can define two distinct dynamic structure factors or electric field correlation functions using these components of the scattered field.

Interface induced anisotropy was developed at the liquid-air interface whereas it was absent at the liquid-liquid interface

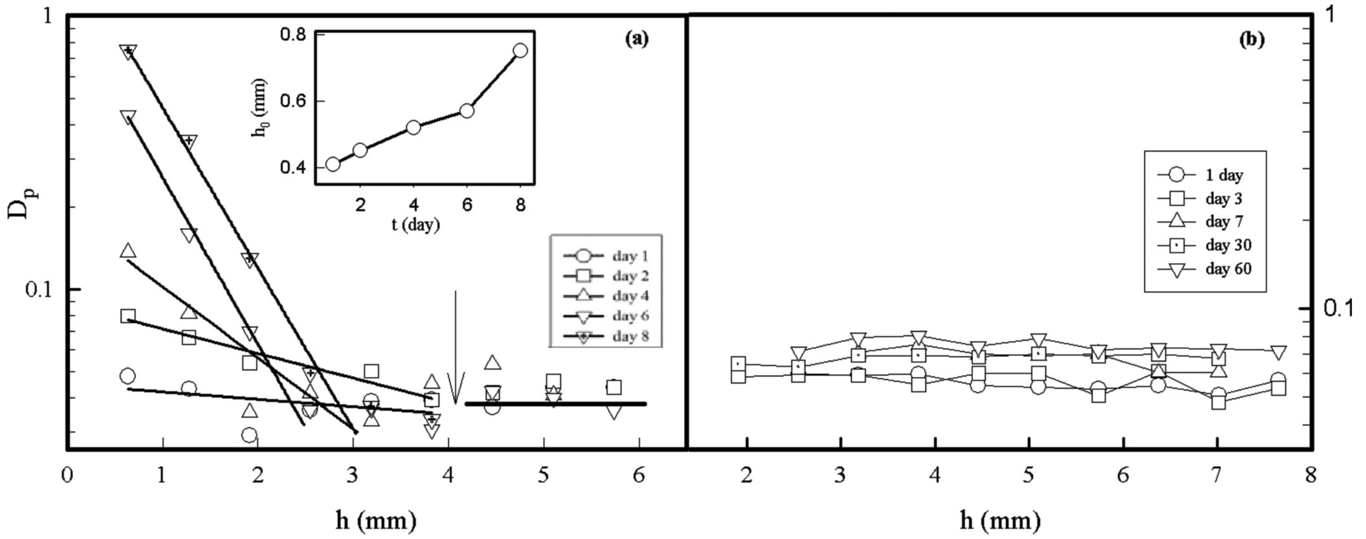

FIG. 2. Variation of depolarization ratio D_p as a function of depth from water-air interface of the sample at different aging times. Panels (a) and (b) depict data for 3% and 1.5% (w/v) dispersions, respectively. The data in (a) were least-squares fitted to the exponential decay given by Eq. (3) (with $\chi^2 = 0.99$), and the decay lengths are plotted as a function of waiting time shown in the inset. The arrow divides the exponential fitting and the constant values. The size of the symbol represents the error in the measurement.

which will be discussed later. Growth in optical anisotropy was monitored systematically with aging time and with depth of the sample. Initially, we had used 3% (w/v) of Laponite to study the anisotropic growth. Figure 2 illustrates a nice evolution of depolarization ratio with depth. A similar observation was made by Shahin *et al.* [26], where they used optical birefringence measurements to find the interface induced ordering. The solid concentration of 3% (w/v) belongs to the glassy state of the Laponite system. The system in glass phase not only undergoes aging but develops spatial ordering which starts at the interface between liquid and air, and percolates into the bulk which is clearly seen from Fig. 2. The depolarization ratio which defines the anisotropic ordering of the system was found to grow with aging and depth of the sample.

Initially the growth in D_p was slow while at long time scales it was rapid. In Fig. 2, D_p is shown as a function of the depth of the sample. It is evident from this plot that there was substantial development of anisotropy at the interface which progressively propagated into the bulk and it vanished slowly beyond the depth of 5 mm. The ordering that was observed in this system was irreversible with aging and depth. Samples with 3% (w/v) of Laponite are assumed to be in the glassy state because these can be melted by dilution.

A strong dependence of D_p on depth h was noticed and an exponential decay behavior could be established. This is given by

$$D_p \sim \exp(-h/h_0). \tag{3}$$

Here the value of the decay length h_0 increases from 0.4 to 0.75 mm with aging time [see Fig. 2(a)].

Interestingly, there was no development of anisotropy observed at lower concentrations of Laponite. We performed measurements up to 60 days but did not observe any significant change in the value for D_p. A typical depiction of this is illustrated in Fig. 2(b).

The D_p versus aging time t_w data shown in Fig. 3 could be least-squares fitted to a power-law function for a given depth h from the interface given by

$$D_p \sim t_w^n. \tag{4}$$

The power-law exponent n increased from 0.1 to 4.0 as one moved away from the interface into the bulk.

B. Effect of water-hydrophobic liquid interface

A very interesting observation was made during our investigations which clearly illustrated the role played by the interface in causing anisotropic ordering of the platelets. In this study, we spread a thin layer of the water immiscible hydrophobic solvent hexanol (also octanol) on the surface of the dispersion, thereby

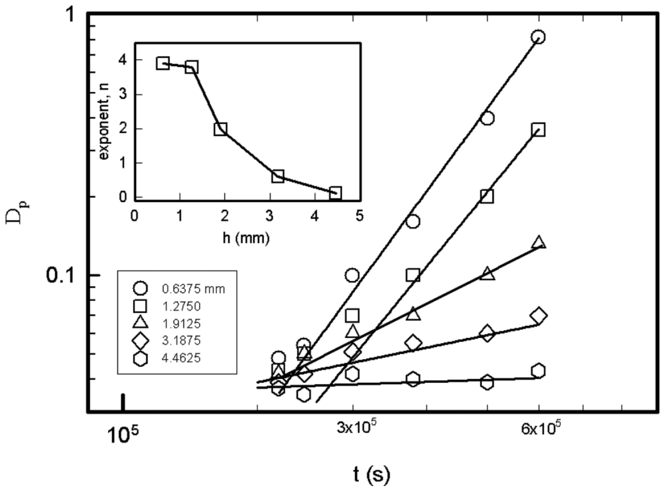

FIG. 3. Time dependent evolution of D_p at various depths of 3% (w/v) Laponite dispersion. These data were least-squares fitted to the power-law relations given by Eq. (4). Inset shows the variation of power-law exponent with depth from interface.

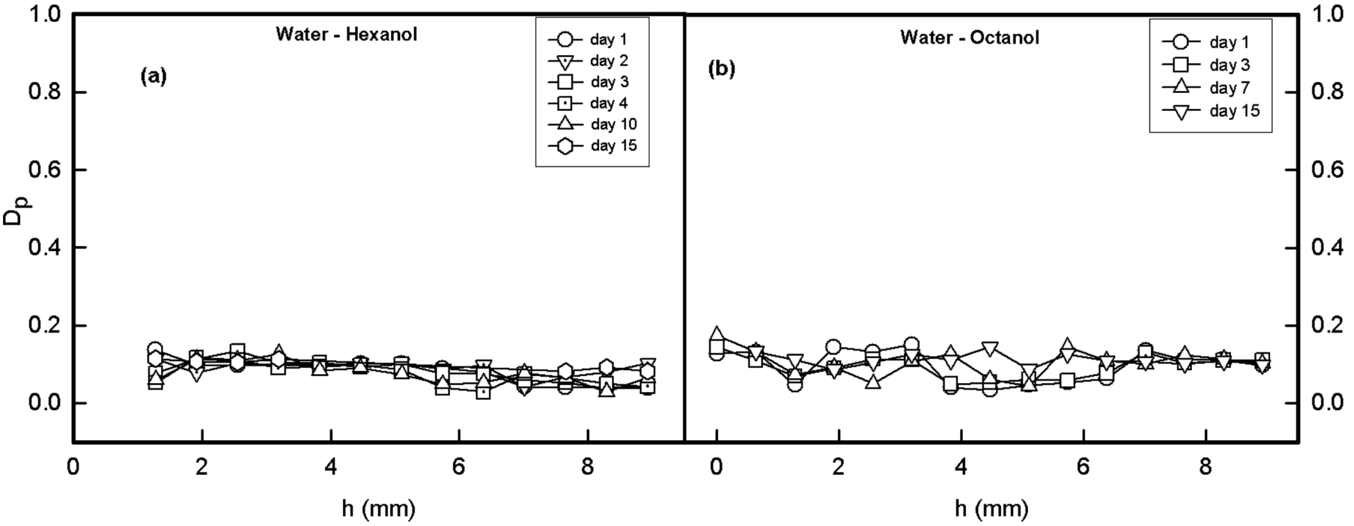

FIG. 4. Effect of covering the surface of the Laponite dispersion with hydrophobic solvent layers. D_p is shown as function of depth at different aging times; (a) water-hexanol and (b) water-octanol interface.

changing the water-air interface to a water-hexanol interface. Surprisingly, no growth in anisotropy was observed in both the cases even at the longer times, though the samples entered the nonequilibrium state (glass). This result is depicted in Fig. 4 pertaining to the two cases where hexanol and octanol layers present on the Laponite dispersion provided the water-hexanol and water-octanol interface, respectively.

C. Effect of temperature

We felt it was imperative to examine whether temperature had any role to play in the ordering of the platelets. There was no enhancement or improvement of ordering in the hydrophobic liquid covered surfaces. For the samples having a water-air interface the effect of temperature induced ordering was observed. This was similar to the one we had observed in our previous study on mixed clay dispersions where the temperature induced ordering in the bulk of the sample was observed [23]. Figure 5 describes the effect of temperature on sample anisotropy for different depths.

The depolarization ratio was observed to decay exponentially as shown in Eq. (3), where h_0 represents the typical decay length. The value of h_0 thus obtained was found to increase with temperature as shown in the inset of Fig. 5, and could follow a power-law behavior given by

$$h_0 \sim T^{\gamma}, \tag{5}$$

where $\gamma = 2.0 \pm 0.2$.

D. Relaxation dynamics

The relaxation dynamics of the system was studied using dynamic light scattering measurements. We have analyzed the dynamic structure factor data both in the polarized and depolarized mode. The dynamic structure factors thus obtained were plotted as shown in Fig. 6 and analyzed using the same protocol that is described in our previous work [20]. We have taken the heterodyne contribution into account while dealing with these nonergodic samples.

The dynamic structure factor $g_1(q,t)$ could be described as

$$g_1(q,t) = a e^{-(t/\tau_1)} + (1-a) e^{-(t/\tau_2)^{\beta}}, \tag{6}$$

where a and $(1-a)$ are the weights of the two contributions τ_1 and τ_2, which in turn are the fast and the slow mode relaxation times, respectively, and β is the stretching parameter. The fast mode relaxation time τ_1 is related to the inverse of the short-time diffusion coefficient D_s as $\tau_1 = 1/D_s q^2$. The presence of stretched exponential function has been reported in the past for clay dispersions, since it has been found empirically that it provides effective description of the slow mode relaxation processes found in arrested systems [12,13,16,20]. Equation (6) gave a good description for both the polarized and the depolarized dynamic structure factors $g_1^{VV}(q,t)$ and $g_1^{VH}(q,t)$.

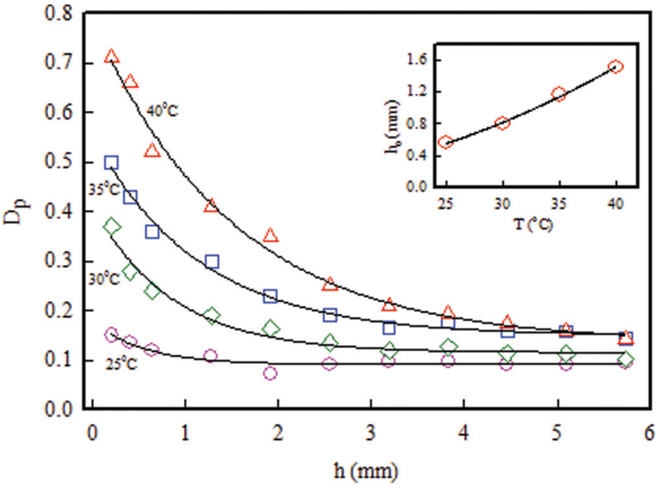

FIG. 5. (Color online) Depolarization ratio shown as a function of depth of the sample at different temperatures as indicated against each curve. This data was least-squares fitted to the exponential relation given by Eq. (3). Inset shows the variation of h_0 as the function of temperature. The solid curves represent the least square fitting to Eq. (5).

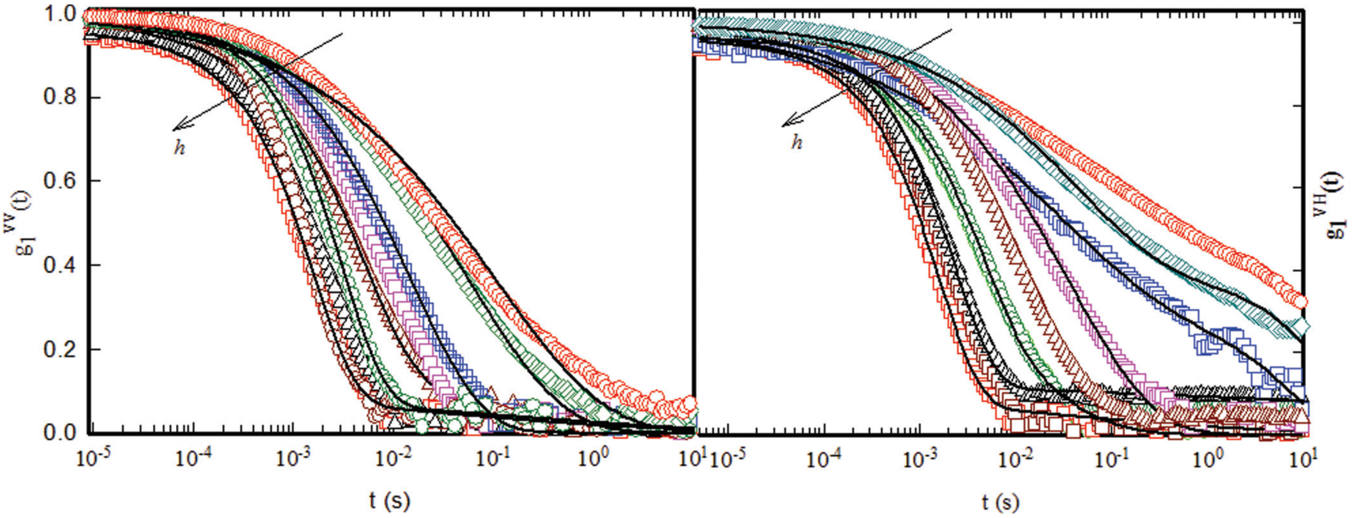

FIG. 6. (Color online) Evolution of the dynamic structure factors, $g_1^{VV}(q,t)$ (left panel) and $g_1^{VH}(q,t)$ (right panel), at different depths at 25 °C. The arrows indicate increasing depths starting from 0.63 to 4.5 mm. Solid lines represent the fitting curve to Eq. (6).

The slow mode relaxation times of both the components are compared in Fig. 7 for results obtained at different temperatures. This relaxation time τ_2 was observed to freeze early at the interface compared to the same in the bulk because the self-arrested structures relax slowly close to the water-air interface. It is interesting to note that the relaxation time of polarized and depolarized complements behaved differently. The slow mode relaxation time τ_2 of $g_1^{VV}(q,t)$ was lower than that of the other component $g_1^{VH}(q,t)$. The τ_2 values obtained were constant beyond the depth of 4 mm. The influence of temperature on this system was also studied and the data are shown in Fig. 7. Measurements were done at 25 °C and 35 °C, which indicated that at higher temperature the system relaxes slowly. The τ_2's obtained from data were compiled and the same are compared for different temperatures, which is shown in Fig. 7.

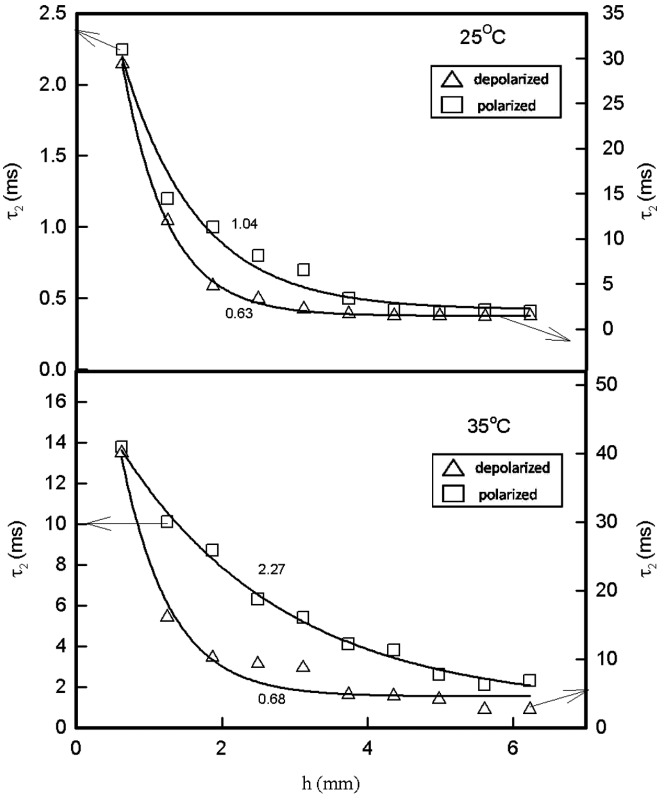

FIG. 7. Characteristic slow mode relaxation time plotted as a function of depth for polarized and depolarized components at different temperatures as indicated. The exponential decay lengths are indicated for each curve.

The slow mode relaxation in both the polarized and depolarized modes decays exponentially with depth of the sample, given as

$$\tau_2 \sim \exp(-h/h_0), \tag{7}$$

where h_0 represents the decay length. The parameter h_0 increases with the temperature as is shown in Fig. 8(a). The stretching parameter β increases as we go from interface into bulk which is shown in Fig. 8(b); this implies that part of interface reached the arrested state much before the same occurred in the bulk.

It reveals that even after slowing down of the dynamics, the particles still have some freedom to move and reorganize themselves in the process of attaining equilibrium. To realize any possible correlation existing between the ordering and the relaxation times we have plotted D_p as function of τ_2 at particular depths. We found a scaling behavior could be found between D_p and τ_2 given as

$$D_p \sim \tau_2^{\alpha}. \tag{8}$$

Temperature dependence α is shown in Fig. 9 for polarized and depolarized components. The value of α was found to increase with temperature.

IV. DISCUSSION

Let us discuss our results in the light of the reported literature in order to get some physical insight. The estimation of surface excess energy through the Gibbs adsorption equation is normally made from the measurement of change in surface tension of solutions containing surface-active molecules as a function of solute concentration. The magnitude of the interaction force depends on, among other things, the particle

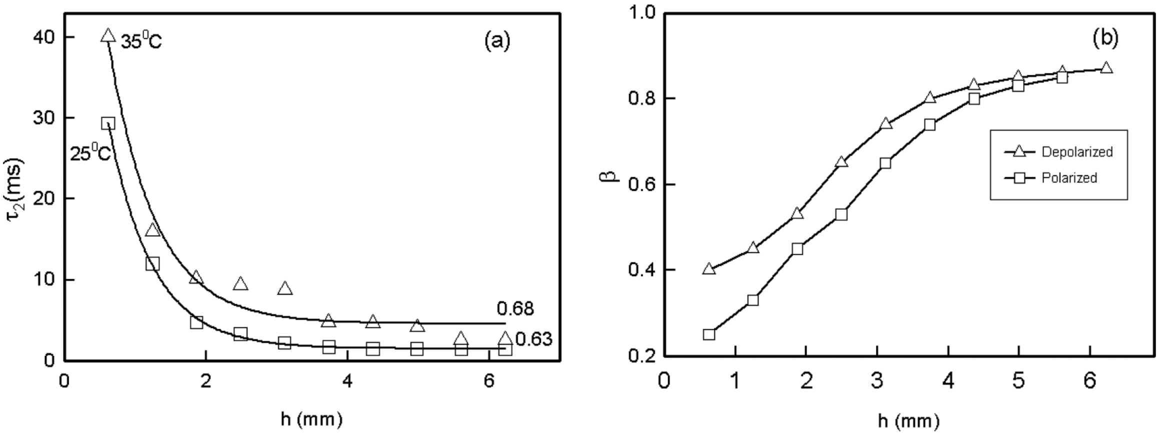

FIG. 8. (a) The characteristic slow mode relaxation time with the depth of the sample at two different temperatures, 25 °C and 35 °C, in the depolarized mode dynamic structure factor, $g_1^{VH}(q,t)$. The exponential decay lengths are indicated for each curve. (b) Depth dependent evolution of β for polarized and depolarized modes at 25 °C.

shape [33]. However, such measurements resulting from colloidal partitioning are not always amenable to experimental probing [34]. Studies indicate that the ordering or partitioning of colloidal suspensions at the water-air interface is strongly influenced by the following factors: (i) colloidal charge, (ii) colloidal size and shape, (iii) aging time, and (iv) temperature. Wang and Tokunaga have reported colloidal partitioning at the water-air interface in a variety of dispersions, and found that the interface was negatively charged under all test conditions (ionic strength, pH, etc.) [34]. For instance, the zeta potential of the interface for de-ionized water-air was −64 mV, whereas in the presence of NaCl (<0.1 M) it ranged between −10 and −90 mV decreasing with increasing pH but increasing with increasing ionic strength [34]. In light of the above, it is pertinent to peruse some reported results. Positively charged polystyrene latex spheres exhibited partitioning at the interface whereas negatively charged spheres revealed no such behavior. Thus, surface exclusion could be ascribed to the electrostatic attraction between the negatively charged interface and positively charged particles. In kaolinite, one of the mineral clays which has a negatively charged surface and positively charged rim, partitioning was observed nonetheless. This was due to the presence of positively charged edge sites that sorbed normal to the interface [34]. Thus, despite the negatively charged face of the clay platelet repelling the similarly charged water-air interface, surface exclusion occurred. In comparison to this the smectite clay montmorillonite (MMT) does not show partitioning because of a much higher face charge that causes substantial repulsion with the negatively charged interface. Further, spillover of the negative electric field from their face surfaces over their thin edges hinders surface exclusion. Thus, surface exclusion in clay dispersions is a function of edge charge, intrinsic charge, and particle aspect ratio.

Let us analyze our experimental results in light of the aforesaid observations. The growth in anisotropy was clearly observed from the depolarization ratio measurements and this increased with aging. We have noticed that relaxation time increased with temperature. Figure 7 suggests that the relaxation time evolves rather slowly at higher temperature. It could be due to the growing repulsive interaction between

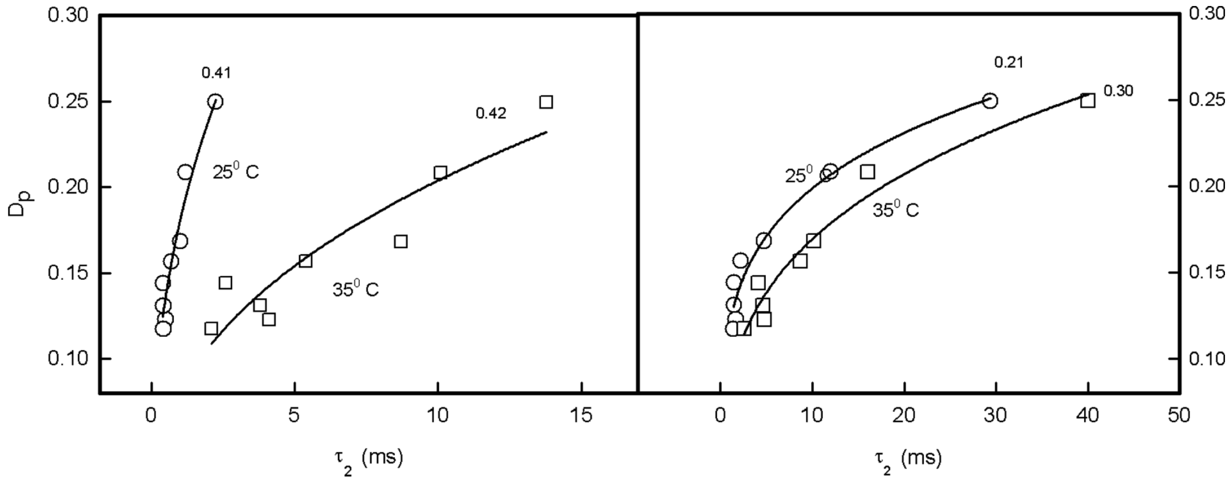

FIG. 9. Depolarization ratio plotted as the function of slow mode relaxation time determined from polarized mode dynamic structure factor, $g_1^{VV}(q,t)$ (left panel), and depolarized mode dynamic structure factor, $g_1^{VH}(q,t)$ (right panel). The power-law exponents are indicated for each curve.

the platelets. From the analysis of the relaxation dynamics it was observed that the particles at the water-air interface were arrested earlier than the particles in the bulk which could occur from the surface exclusion effect. Further, the relaxation time of the depolarized component decayed faster than the polarized component. Thus, we could clearly observe the presence of heterogeneity in the aging samples varying with depth measured from the interface. Mamane *et al.* made a very interesting observation on the surface fluctuations of an aging Laponite suspension [35]. They showed that as the dispersion aged, the dynamics became heterogeneous and those quakes at the surface were uncorrelated. It was shown that, at large enough waiting times, the thermally induced surface fluctuations exhibited bursts of activity, and were characterized by non-Gaussian dynamics. Further, the corresponding events induced large changes in the local slope of the free surface at a scale several decades larger than the particle size and were uncorrelated. In that process particles tried to attain the minimum free energy configuration by arranging themselves with their major axis parallel to the interface.

Our measurements found the existence of correlation between the ordering and the structural relaxation time with aging and with depth measured from the interface. Moreover dilution destroyed the ordering, implying the presence of a strong repulsive interaction between the platelets as shown in Fig. S1 in the Supplemental Material [36]. The growth of viscosity as a function of temperature is shown in Fig. S2 [36]. Thus, the anisotropic phase could be identified as orientationally ordered glass of colloidal platelets. But when the surface of the dispersion was covered with a thin layer of hydrophobic solvent, anisotropic ordering was not observed. Even high temperature was not able to drive the system to cause the anisotropic ordering.

The general issue of the microstructure of liquid-air or liquid-liquid interface and its complex dynamics is still a topic of intense debate. The thickness of the liquid-liquid (water-alcohol) interface is considered to be only a few nanometers [37,38]. These interfaces are flexible and cannot be fixed at a given spatial position. For the water-air interface measurements one may be tempted to propose that the interface is responsible for the ergodicity breaking, but it may not be the case. The water-alcohol interface is not entirely resisting the system from going into the arrested state. It could be possible that the octanol-water interface was acting like a reflecting boundary not allowing the particles to order, stay, or stick at the interface for longer times. The conceptualization of the physical picture of interface driven ordering, surface exclusion, and partitioning requires further investigations.

V. CONCLUSION

We have studied the relaxation dynamics of the interface dependent ordering phenomenon systematically using the light scattering experiments. The geometry that we have used in our experiments conclusively mapped the dynamics of anisotropy growth occurring at the interface and propagating into the bulk with aging. We believe that the water-air interface is responsible for causing this ordering. The density fluctuations at the interface of water and air are much stronger compared to the bulk, which may be responsible for the observed occurrence of anisotropy. The parameters that enhanced the ordering were the aging time and temperature. The higher the temperature, the higher was the amount of depolarization, and the particles encountered the arrested state early. Interestingly, we noticed the presence of heterogeneous relaxations in these dispersions that varied with the depth which was not seen hitherto. In this work we found the existence of a correlation between the ordering and the relaxation times with depth of the sample from the interface, aging, and temperature. When the interface surface was covered with oil or water immiscible liquids, the surface fluctuations vanished and the dynamics of aging exhibited homogeneous features. Interestingly the covering of the surface has a significant effect on the arrested dynamics. The ergodicity breaking time is delayed when the surface is covered with water immiscible liquids, and the examinations in this direction are underway. We infer that pH and salt dependence have to be studied in this system to gain further insight into the ordering phenomenon.

ACKNOWLEDGMENTS

R.K.P. acknowledges support through a Senior Research Fellowship from the Council of Scientific and Industrial Research, Government of India. This work was supported by a research grant from Department of Science and Technology, Government of India.

---

[1] H. H. Wickman and J. N. Korley, Nature **393**, 445 (1998).

[2] H. K. Choi, M. H. Kim, S. H. Im, and O. O. Park, Adv. Funct. Mater. **19**, 1594 (2009).

[3] Z. Chen, L. Baird, and L. Tan, J. Phys. Chem. B **117**, 2807 (2013).

[4] E. C. Mbamala and H. H. von Grünberg, Phys. Rev. E **67**, 031608 (2003).

[5] M. Dijkstra, J. P. Hansen, and P. A. Madden, Phys. Rev. Lett. **75**, 2236 (1995).

[6] D. Bonn, H. Tanaka, G. Wegdam, H. Kellay, and J. Meunier, Europhys. Lett. **45**, 52 (1999).

[7] P. Coussot, Q. D. Nguyen, H. T. Huynh, and D. Bonn, Phys. Rev. Lett. **88**, 218301 (2002).

[8] B. Ruzicka, L. Zulian, and G. Ruocco, Phys. Rev. Lett. **93**, 258301 (2004).

[9] B. Abou and F. Gallet, Phys. Rev. Lett. **93**, 160603 (2004).

[10] H. Z. Cummins, J. Non-Cryst. Solids **353**, 3891 (2007).

[11] B. Ruzicka, E. Zaccarelli, L. Zulian, R. Angelini, M. Sztucki, A. Moussaïd, T. Narayanan, and F. Sciortino, Nat. Mater. **10**, 56 (2011).

[12] S. Jabbari-Farouji, E. Eiser, G. H. Wegdam, and D. Bonn, J. Phys. Condens. Matt. **16**, L471 (2004).

[13] B. Ruzicka, L. Zulian, and G. Ruocco, Langmuir **22**, 1106 (2006).

[14] R. K. Pujala, N. Pawar, and H. B. Bohidar, Langmuir **27**, 5193 (2011).

[15] A. Shahin and Y. M. Joshi, Langmuir **28**, 5826 (2012).
[16] S. Jabbari-Farouji, G. H. Wegdam, and D. Bonn, Phys. Rev. E **86**, 041401 (2012).
[17] B. Ruzicka, L. Zulian, and G. Ruocco, J. Phys.: Condens. Matter **16**, 4993 (2004).
[18] A. Shahin and Y. M. Joshi, Langmuir, Phys. Rev. Lett. **106**, 038302 (2011).
[19] A. Shahin and Y. M. Joshi, Langmuir **26**, 4219 (2010).
[20] R. K. Pujala and H. B. Bohidar, Soft Matter **8**, 6120 (2012).
[21] R. K. Pujala and H. B. Bohidar, Soft Matter **9**, 2003 (2013).
[22] E. L. Hansen, H. Hemmen, D. M. Fonseca, C. Coutant, K. D. Knudsen, T. S. Plivelic, D. Bonn, and J. O. Fossum, Sci. Rep. **2**, 618 (2012).
[23] R. K. Pujala, N. Pawar, and H. B. Bohidar, J. Chem. Phys. **134**, 194904 (2011).
[24] H. van Olphen, *An Introduction to Clay Colloid Chemistry* (John-Wiley, New York, 1977).
[25] *Laponite Technical Bulletin*, LI04/90/A, Laponite Industries Limited (1990).
[26] A. Shahin, Y. M. Joshi, and S. A. Ramakrishna, Langmuir **27**, 14045 (2011).
[27] B. J. Lemaire, P. Panine, J. C. P. Gabriel, and P. Davidson, Europhys. Lett. **59**, 55 (2002).
[28] A. Mourchid, A. Delville, J. Lambard, E. LeColier, and P. Levitz, Langmuir **11**, 1942 (1995).
[29] C. Martin, F. Pignon, A. Magnin, M. Meireles, V. Leliãvre, P. Lindner, and B. Cabane, Langmuir **22**, 4065 (2006).
[30] F. Pignon, M. Abyan, C. David, A. Magnin, and M. Sztucki, Langmuir **28**, 1083 (2012).
[31] B. Ruzicka and E. Zaccarelli, Soft Matter **7**, 1268 (2011).
[32] B. J. Berne and R. Pecora, *Dynamic Light Scattering with Applications to Chemistry, Biology and Physics* (Wiley-Interscience, New York, 1976).
[33] S. Aramrak, M. Flury, J. B. Harsh, R. L. Zollars, and H. P. Davis, Langmuir **29**, 5770 (2013).
[34] J. Wan and T. K. Tokunaga, J. Colloid Interface Sci. **247**, 54 (2002).
[35] A. Mamane, C. Fretigny, F. Lequeux, and L. Talini, Europhys. Lett. **88**, 58002 (2009).
[36] See Supplemental Material at http://link.aps.org/supplemental/10.1103/PhysRevE.88.052310 for the variation in D_p with dilution of the 3% (w/v) Laponite at different times and the evolution of viscosity as a function of temperature.
[37] D. M. Mitrinovic, Z. Zhang, S. M. Williams, Z. Huang, and M. L. Schlossman, J. Phys. Chem. B **103**, 1779 (1999).
[38] J. Gao and W. L. Jorgensen, J. Phys. Chem. **92**, 5813 (1988).